Design and mechanical properties of supramolecular polymeric materials based on host-guest interactions: the relation between relaxation time and fracture energy

Journal:	*Polymer Chemistry*
Manuscript ID	PY-ART-09-2020-001347
Article Type:	Paper
Date Submitted by the Author:	24-Jun-2020
Complete List of Authors:	Konishi, Subaru; Osaka University Graduate School of Science Department of Macromolecular Science Kashiwagi, Yu; Osaka University Graduate School of Science Department of Macromolecular Science Watanabe, Go; Kitasato University, Physics Osaki, Motofumi; Graduate School of Science, Osaka University, Department of Macromolecular Science Katashima, Takuya; The University of Tokyo, Graduate School of Engineering, Depart of Materials Engineering Urakawa, Osamu; Osaka University, Department of Molecular Science Inoue, Tadashi; Osaka University, Macromolecular Science Yamaguchi, Hiroyasu; Osaka University, Department of Macromolecular Science, Graduate School of Science Harada, Akira; Osaka University Graduate School of Science Department of Macromolecular Science, Takashima, Yoshinori; Graduate School of Science, Osaka University, Department of Macromolecular Science; Institute for Advanced Co-Creation Studies,

ARTICLE

Received 00th January 20xx,
Accepted 00th January 20xx

DOI: 10.1039/x0xx00000x

Design and mechanical properties of supramolecular polymeric materials based on host-guest interactions: the relation between relaxation time and fracture energy

Subaru Konishi,[a] Yu Kashiwagi,[a] Go Watanabe,[b] Motofumi Osaki,[a,c] Takuya Katashima,[d] Osamu Urakawa,[a] Tadashi Inoue,[a,c] Hiroyasu Yamaguchi,[a,c] Akira Harada,*[e] and Yoshinori Takashima*[a,c,f]

Functional polymeric materials based on reversible noncovalent bonds have attracted much attention due to their mechanical and responsive properties. In particular, the association/dissociation of the reversible bond is widely known to improve the fracture energy of polymeric materials. Herein, we aimed to establish a general strategy for designing tough materials and investigated the relation between the lifetime of reversible bonds and the toughness of the material. We experimentally demonstrated the fracture energy in relation to the viscoelastic relaxation time (τ) of the reversible bonds and the observation time scale. We prepared supramolecular hydrogels cross-linked by inclusion complexes between α-cyclodextrin (αCD) and alkyl chains modified with cation units. τ varied widely in response to the kinetics of the threading/dethreading of the αCD unit. The viscoelastic behaviour of the reversible cross-linking points, which could be tuned by τ and the tensile rate, improved the fracture energy of the supramolecular hydrogels.

1. Introduction

Polymeric gels[1–3] containing solvent are utilized in various fields.[4–7] However, compared to natural hydrogels (cartilage and polysaccharides *etc*.), synthetic hydrogels are usually weak or brittle, which limits their range of applications.[8,9] Substantial developments in mechanical properties have been made in the field of polymeric materials by adopting new kinds of material designs,[9–11] such as multiple network gels,[12–18] nanocomposite gels,[19–25] polyrotaxane gels,[26–28] slide-ring gels,[29–33] rotaxane cross-linked gels,[34–36] and ideal polymer networks.[37,38] The reversible cross-linking of polymer chains is also well suited for preparing functional materials.[10,39,40] Reversible cross-linkers consist of dynamic covalent bonds[41] or noncovalent bonds, including ionic interactions,[42–46] coordination bonds,[47] hydrogen bonds,[48,49] hydrophobic interactions,[50,51] and host-guest interactions.[52–61] Depending on the chemical properties of the bonds or interactions, hydrogels can exhibit self-healing, stimuli-responsiveness, shape-memory, controlled mechanical properties, and so on. In particular, the association/dissociation of reversible cross-links under stress commonly dissipates the stress, which improves fracture energy. These physical properties of hydrogels are intricately affected by many parameters in reversible cross-linking, such as the association constant, activation energy, relaxation time of the bonds, and cross-linking density. These factors are controllable and can be tuned by changing the molecular shape and the main chain polymer. Investigating the effects of various factors on the physical properties should contribute to a universal design for functional materials.

Cyclodextrins (CDs) are well known as host molecules that can include hydrophobic guest molecules in their cavity.[62,63] Host-guest complexes of CD have been utilized as cross-linking structures to achieve functional polymeric materials.[58,59,64] Previously, we employed *pseudo*-rotaxane as a cross-linker between CD and an alkyl-viologen polymer (VP; alternate copolymer of alkyl chains and viologen cations).[65] CDs are difficult to include cationic units in their cavities due to their electric instability, where cationic species prevent CD from threading/dethreading along the alkanediyl axis.[66–70] Therefore, cations kinetically control the threading/dethreading of CDs with the axis molecules. Bulky groups at ends of axis molecules also decrease the threading/dethreading rate.[68,71,72]

The threading/dethreading rate of αCD onto VP is very slow on the NMR time scale, exhibiting two split signals derived from the inclusion complexes and the free species, but the rate of βCD is not as slow.[73] An αCD dimer with VP forms a main-chain-

---

[a] Department of Macromolecular Science, Graduate School of Science, Osaka University. 1-1 Machikaneyama-cho, Toyonaka, Osaka 560-0043 (Japan). E-mail: takasima@chem.sci.osaka-u.ac.jp
[b] Department of Physics, School of Science, Kitasato University. 1-15-1 Kitasato, Minami-ku, Sagamihara, Kanagawa 252-0373 (Japan).
[c] Project Research Center for Fundamental Sciences, Osaka University. 1-1 Machikaneyama-cho, Toyonaka, Osaka 560-0043 (Japan).
[d] Department of Bioengineering, School of Engineering, The University of Tokyo. 7-3-1 Hongo, Bunkyo-ku, Tokyo 113-8656 (Japan).
[e] The Institute of Scientific and Industrial Research, Osaka University. 8-1 Mihogaoka, Ibaraki, Osaka 560-0047 (Japan). E-mail: harada@chem.sci.osaka-u.ac.jp
[f] Institute for Advanced Co-Creation Studies, Osaka University. 2-1 Yamada-oka, Suita, Osaka 565-0871 (Japan). E-mail: takasima@chem.sci.osaka-u.ac.jp

† Electronic Supplementary Information (ESI) available. See DOI: 10.1039/x0xx00000x

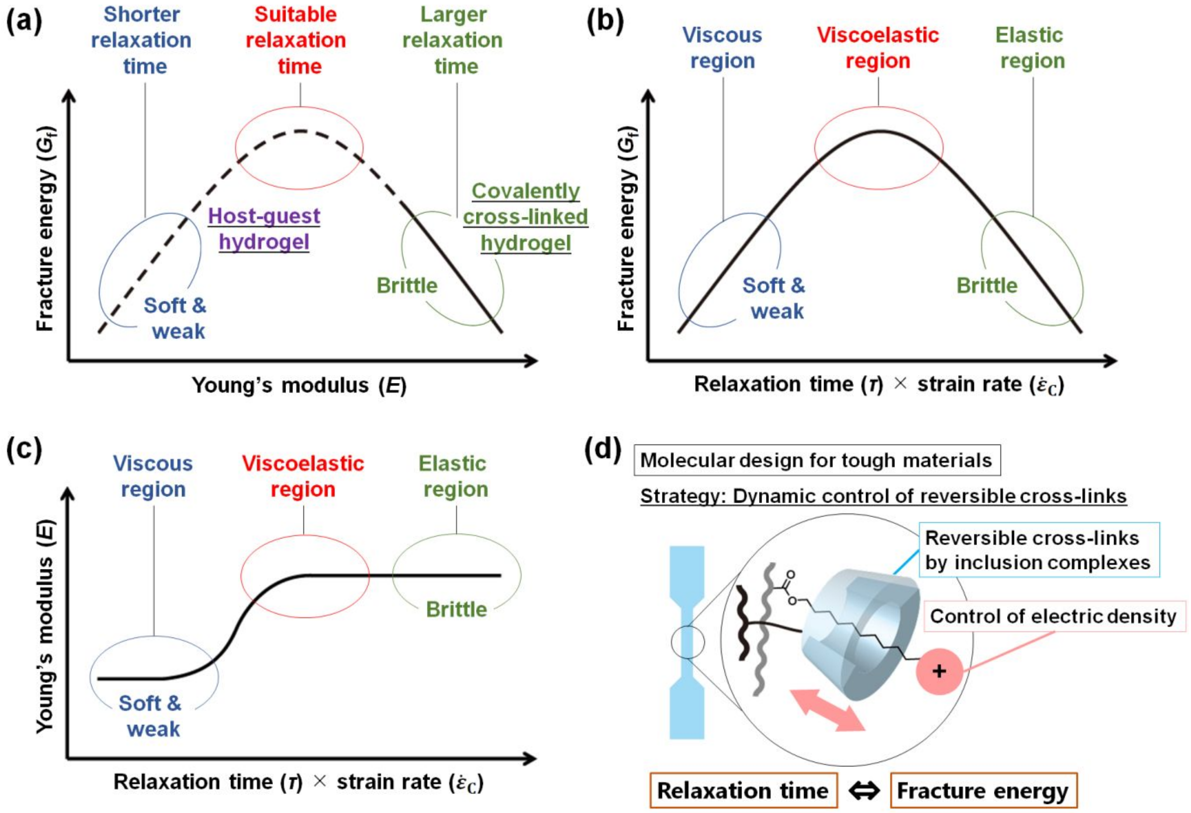

Figure 1. Design concept of supramolecular hydrogels. **(a)** Trend between fracture energy (G_f) and Young's modulus (E) of viscoelastic hydrogels with various relaxation times. **(b)** Dependence of G_f on viscoelasticity. **(c)** Dependence of E on viscoelasticity. **(d)** Schematic of the reversible cross-linking points in these materials.

type supramolecular hydrogel, but the βCD dimer does not give similar signals due to the fast exchange rate and short viscoelastic relaxation time (τ).[65] Hydrogelation is related to the relaxation time of the cross-linking point with the CD dimers. The rates of association and dissociation depend on the energy barrier of the CD host unit passing over the axis. Similar association/dissociation behaviour has been observed in side-chain-type supramolecular hydrogels.[74] The CD cavity size and shape and the charge of the guest unit affect the mechanical properties of the material. To improve the mechanical properties of CD-based supramolecular hydrogels, we should establish fundamental material design principles.

Based on previous works, the combination of host/guest molecules with a high association constant (K_a) did not give supramolecular hydrogels with a high fracture energy (G_f), but the Young's modulus (E) of the hydrogel at a certain strain rate was increased.[74] On the other hand, increasing the charge at the end of the alkyl guest unit effectively improved G_f, which is closely related to the kinetics of the threading/dethreading of the CD units. Here, we hypothesize that τ can be tuned to control G_f and E in host/guest supramolecular hydrogels. Actually, dynamics of reversible cross-linking point are well known to have an impact on dynamics and mechanics of transient polymer networks.[60,75–79] Figure 1a shows the trend between G_f and E in viscoelastic materials. As hydrogels with low E show low stress values, G_f should decrease. In contrast, high E should result in very small fracture strain and a small G_f. This trend corresponds to the behaviour of the covalently cross-linked hydrogels, G_f of which is generally proportional to $E^{-1/2}$ (the Lake-Thomas model).[80–82] A suitable E would give materials with the highest G_f. From the viewpoint of viscoelastic dynamics, if the hydrogel behaves as a viscous body with low $\tau \times \dot{\varepsilon}_C$ ($\dot{\varepsilon}_C$: strain rate), G_f should decrease due to the low loss modulus (G''). In the case of an elastic body with a high $\tau \times \dot{\varepsilon}_C$, G_f also decreases because of the low G''. If host/guest supramolecular hydrogels with viscoelastic properties and a maximum G'' are prepared by tuning $\tau \times \dot{\varepsilon}_C$, we will obtain materials with the highest G_f (Figure 1b). Of course, E is also related to $\tau \times \dot{\varepsilon}_C$ (Figure 1c). At $\tau \times \dot{\varepsilon}_C > 1$, E significantly increases to a steady state.

Herein, we studied the relationship between the τ value of the reversible bonds and G_f in supramolecular hydrogels. To control the τ value, we designed a reversible cross-linking point using CDs, alkyl chains, and cations (Figure 1d). We revealed the relationship between G_f and E with $\tau \times \dot{\varepsilon}_C$, which will facilitate the design of tough materials.

2. Results and Discussion

2-1. Preparation of the αCD-R hydrogels with cationic guest molecules

We prepared five kinds of reversibly cross-linked supramolecular hydrogels (αCD-R hydrogels), αCD-C12, αCD-ImC11, αCD-PyC11, αCD-VC11 and αCD-TMAmC11 hydrogels (Figures 2a and 2b). The αCD-R hydrogels have cation-

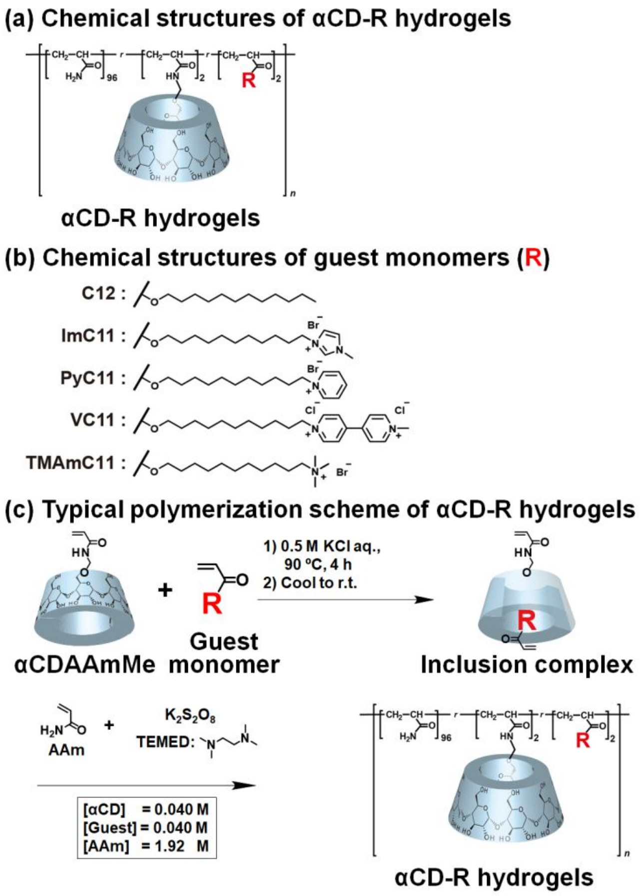

Figure 2. (a) Chemical structures of the αCD-R hydrogels. **(b)** Chemical structures of the guest monomers. **(c)** Typical polymerization scheme for the αCD-R hydrogels.

terminated or nonion linear alkyl chain guests on the polymer side chain. Figure 2b shows the chemical structures of the cationic guest units. The linear alkyl chain units function as a molecular recognition sites for αCD. The cationic groups function as electric traps.[69] The guest units of the αCD-C12 hydrogel have no cationic units. The αCD-ImC11 and αCD-PyC11 hydrogels have imidazolium and pyridinium (monocation) units, respectively. Viologen (dication) units were introduced into the αCD-VC11 hydrogel to increase the electric density. The αCD-TMAmC11 hydrogel have bulky trimethylammonium (monocation) units that show the effect of steric hindrance on αCD.[71] The increase in the electric density or steric hindrance on the cationic moiety decreases the kinetic rate in the association/dissociation equilibrium of the αCD/R complex.

Prior to radical copolymerization to obtain the αCD-R hydrogels, the αCD monomer (αCDAAmMe, 2 mol%, 40 mmol/L) and cation-terminated guest monomers (2 mol%, 40 mmol/L) were stirred in 0.5 M potassium chloride (KCl) aqueous solution to form the inclusion complexes. KCl prevented ImC11, PyC11, and VC11 monomers from precipitating when the redox initiator was added. To confirm the formation of the inclusion complex of αCDAAmMe with ImC11, PyC11, or VC11 monomers, 1D nuclear magnetic resonance (NMR) and 2D ^{1}H rotating-frame Overhauser effect spectroscopy (ROESY) NMR spectra were measured in D_2O. The spectra of αCDAAmMe/ImC11 (Figures S16 and S18a) show that the signals of the protons of the alkyl chain of ImC11 are shifted and broadened. Figures S10–11 show that methylene groups j, k, and l of ImC11 showed ROE correlations to $C^{3,6}H$ and C^5H around the narrow rim of αCDAAmMe, whereas the $C^{2,4}H$ protons showed weak correlations. Similar to αCDAAmMe/ImC11, the signals of alkyl chain protons i, j, and k, of PyC11 are also shifted and broadened (Figure S21a) and are correlated to $C^{3,6}H$ and C^5H in the ROESY spectra of αCDAAmMe/PyC11 (Figures S12–13). The ROESY spectra of αCDAAmMe/TMAmC11 (Figures S14–15) showed a similar result. These results indicate that the alkyl chains of ImC11, PyC11, and TMAmC11 were included in the cavity of αCDAAmMe.

The αCD-R hydrogels were obtained by radical copolymerization according to our previous reports[74,83,84] (Figure 2c). These complex monomers, αCDAAmMe/ImC11, αCDAAmMe/PyC11, αCDAAmMe/VC11, and αCDAAmMe/TMAmC11 were copolymerized with acrylamide (AAm; 96 mol%) at a total monomer concentration of 2 mol/L by using potassium persulfate ($K_2S_2O_4$, 1 mol%) and *N*,*N*,*N*′,*N*′-tetramethylethylenediamine (TEMED, 1 mol%) at room temperature to give the αCD-R hydrogels (Figure 2c, Schemes S4–8, and Tables S1–5). Volume of the materials did not change through polymerization. Therefore, the concentration of the CD and guest units in the hydrogels was 40 mmol/L, where [CD]/[guest]/[main chain] were 2/2/96. Fourier transform infrared (FT-IR) (Figure S23) and ^{1}H field gradient magic angle spinning (FG-MAS) NMR (Figures S24–28) spectroscopic analyses were used to structurally characterize the αCD-R hydrogels. Figures S24–28 show the presence of αCDAAmMe, cationic guest, and AAm units in the αCD-R hydrogel. The protons on the double bond of αCDAAmMe and the cationic

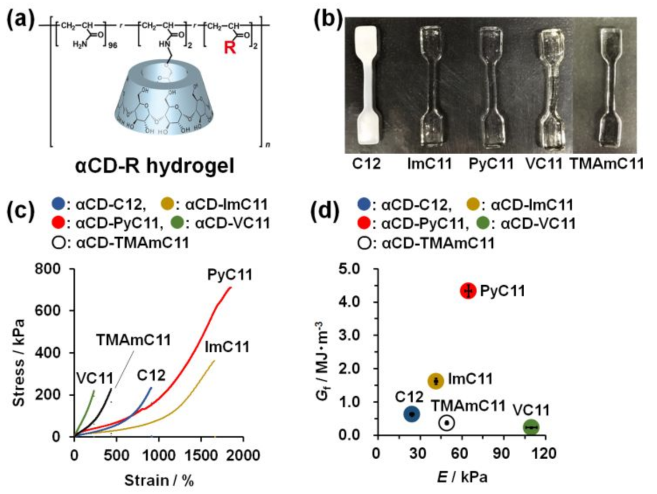

Figure 3. (a) Chemical structure of the αCD-R hydrogels. **(b)** Photograph of the as-prepared αCD-R hydrogels. **(c)** Stress-strain curves of the αCD-R hydrogels at a tensile rate of 1.0 mm/s. **(d)** Plots of fracture energy (G_f) and Young's modulus (E) for the αCD-R hydrogels; αCD-C12 hydrogel: G_f = 0.62 ± 0.05 MJ/m^3 and E = 24 ± 1.4 kPa; αCD-ImC11 hydrogel: G_f = 1.62 ± 0.09 MJ/m^3 and E = 41 ± 1.2 kPa; αCD-PyC11 hydrogel: G_f = 4.33 ± 0.18 MJ/m^3 and E = 64 ± 2.2 kPa; αCD-VC11 hydrogel: G_f = 0.22 ± 0.03 MJ/m^3 and E = 110 ± 4.0 kPa; and αCD-TMAmC11 hydrogel: G_f = 0.37 ± 0.05 MJ/m^3 and E = 49 ± 1.0 kPa.

guest monomers disappeared, indicating that a predefined monomer ratio was introduced into the αCD-R hydrogels.

2-2. Mechanical properties of the αCD-R hydrogels

Uniaxial tensile tests (tensile rate: 1.0 mm/s, 25 °C) were used to evaluate the mechanical properties of the αCD-R hydrogels (Figure 3a–3c). Figure 3b shows a photograph of the αCD-R hydrogels prepared using type 3 dumbbell-shaped Teflon mold following the JIS K6251 standard. The αCD-ImC11, αCD-PyC11, αCD-VC11 and αCD-TMAmC11 hydrogels were transparent, while the αCD-C12 hydrogel was not. The turbidity of the αCD-C12 hydrogel is derived from the microcrystals of the inclusion complex of the αCD/C12 monomers and the formation of the nanosized hydrogel. After polymerization, the obtained αCD-C12 hydrogel had the prescribed αCD/C12 monomer unit ratio. Figure 3c shows typical nominal stress-nominal strain curves of the αCD-R hydrogels. G_f was calculated from the integral of the stress-strain curve, and E was calculated from the initial slope of the stress-strain curve in the range between 3%–8% strain. Figure 3d shows the relation between G_f and E, which varied with the structure of the reversible cross-links. The error bars (standard deviation) were calculated from more than three experiments. The αCD-C12 hydrogel showed low G_f and E. In the cases of the αCD-ImC11 and αCD-PyC11 hydrogels, which had monocationic moieties, both G_f and E were higher than those of the αCD-C12 hydrogel. In particular, the αCD-PyC11 hydrogel exhibited a high G_f (4.33 ± 0.18 MJ/m^3). Unexpectedly, although the charge numbers of the cation species in the ImC11 and PyC11 units were the same, the mechanical properties (G_f and E) of the αCD-ImC11 and αCD-PyC11 hydrogels were significantly different. The αCD-VC11 hydrogel bearing dicationic moieties showed the highest E but the lowest G_f. Similarly, in the case of the αCD-TMAmC11 hydrogel bearing bulky monocationic moieties, E was higher than that of the αCD-C12 hydrogel, but G_f decreased. We wondered why the G_f of the αCD-PyC11 hydrogel was higher than that of the αCD-VC11 hydrogel because the hydrogels have the same alkyl chain length. We suppose that K_a or τ may be major contributors to G_f and E of the αCD-R hydrogels.

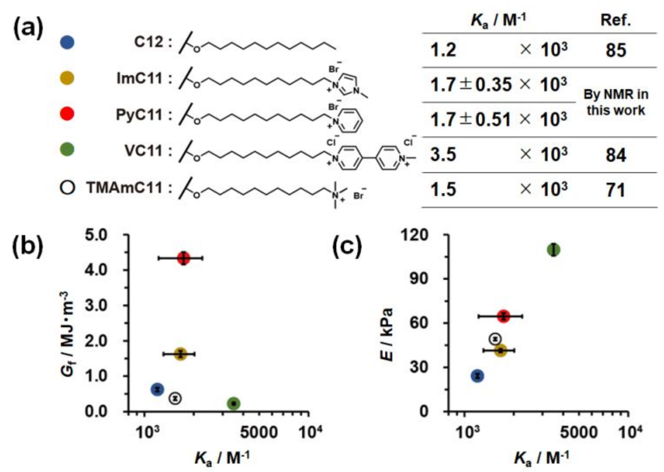

Figure 4. **(a)** Association constants (K_a) of αCDAAmMe with guest units in aqueous solutions. K_a of the αCDAAmMe unit with the C12 unit is 1200 M^{-1} by using αCD and *n*-dodecyl(ester)-acrylamide polymer.[85] Those with ImC11 and PyC11 were determined by NMR in this study (Figures S16–21). That with VC11 was calculated in our previous work.[84] K_a of αCD with N^1,N^1,N^1,N^{10},N^{10},N^{10}-hexamethyldecane-1,10-diaminium (1540 M^{-1})[71] was cited as a model of αCDAAmMe with TMAmC11. **(b)** G_f of the αCD-R hydrogels against K_a. **(c)** E of the αCD-R hydrogels against K_a.

2-3. Relationship between the mechanical properties and association constant

We investigated the effects of K_a between the αCDAAmMe host and the corresponding guest monomers on G_f and E of the αCD-R hydrogels. Figures 4a and S16–21 show the K_a values calculated from the ^{1}H NMR spectra. The resonance peaks of the guest units shifted with the concentration of the αCDAAmMe host monomer. Based on the changes in the chemical shifts, we determined K_a of αCDAAmMe with ImC11, PyC11, and VC11[84] using the nonlinear least-square method. K_a of the αCDAAmMe unit with the C12 unit is 1200 M^{-1} by using αCD and *n*-dodecyl(ester)-acrylamide polymer.[85] K_a of αCD with N^1,N^1,N^1,N^{10},N^{10},N^{10}-hexamethyldecane-1,10-diaminium (1540 M^{-1})[71] was cited as a model of αCDAAmMe with TMAmC11. Figure 4b shows the relation between K_a and G_f. The K_a values of the αCD-C12, αCD-ImC11, αCD-PyC11, αCD-VC11, and αCD-TMAmC11 complexes were in almost the same order in the range of 1.2–3.5 × 10^3 M^{-1}. On the other hand, the αCD-PyC11 hydrogel exhibited a high G_f (4.3 MJ/m^3), but the others showed low G_f values (< 2.0 MJ/m^3) even with the same K_a. This result indicates that K_a does not affect the G_f of the αCD-R hydrogels.

Figure 4c shows the relation between K_a and E of the αCD-R hydrogels. The order of the E values is αCD-C12 < αCD-ImC11 < αCD-TMAmC11 < αCD-PyC11 < αCD-VC11 hydrogels. E is generally proportional to the cross-linking density. To consider the effect of K_a on the cross-linking density of the αCD-R hydrogels, we calculated the complexation ratio using the K_a value and a preset concentration of the host and guest molecules (Figure S22). The theoretical concentration of the inclusion complex in the αCD-R hydrogel was estimated to be 0.035–0.037 mol/L, indicating that the cross-linking density of the αCD-R hydrogels was almost the same. The range of theoretical concentrations of the inclusion complexes was smaller than the range of E values of the αCD-R hydrogels. The above result suggests that the effect of K_a on E was relatively small. Therefore, we hypothesize that the threading/dethreading kinetics of the CD units is mainly affected G_f and E.

2-4. Relation between the mechanical properties and the partial atomic charges of the cationic moieties

To assess the threading/dethreading kinetics of CD units, we evaluated the potential barrier of the cationic species by using charge density analysis. The partial atomic charges on ImC11, PyC11, VC11, and TMAmC11 were calculated using the restrained electrostatic potential (RESP)[86] methodology based on quantum chemical calculations at the B3LYP level using the 6-31G(d,p) basis set in Gaussian 09 Rev. E01[87] (Figures 5a and S37–S40). Figure 5a shows that RESP partial atomic charges on quaternary ammonium cations (N$^+$) increased in the order of ImC11 < TMAmC11 < PyC11 < VC11. The potential barrier (electric instability) between the CD units and the cationic units should increase in the same order.

A clear correlation between the RESP charges on N^+ and the mechanical properties was observed. G_f reached its maximum at a RESP charge of approximately 0.2–0.3 (Figure 5b), indicating that a suitable RESP charge should give the highest G_f. E increased with RESP charge (Figure 5c), indicating that the RESP charge directly affects the stiffness of the αCD-R hydrogels. The RESP charge is closely related to the activation energy of the kinetics of the threading/dethreading CD units. These relations suggest that the kinetics of the threading/dethreading of the CD units, in other words, the lifetime of the reversible cross-links, has a major impact on the G_f and E of the αCD-R hydrogels. It is to be noted that not only the RESP charge but also steric hindrance of the TMAmC11 should influence G_f and E of the αCD-TMAmC11 hydrogel.

2-5. Relaxation behaviours of the αCD-R hydrogels

Rheological analyses were used to determine the relaxation time of the αCD-R hydrogels (Figures S41–45). Figures S41c–45c show the frequency (ω) dependence of the storage modulus (G'), loss modulus (G''), and loss factor (tan δ) at different temperatures, which followed the time-temperature superposition to give the master curves referenced at 25 °C (Figures S41d–45d). Figures S46–49 show the results of the stress-relaxation test of the αCD-VC11 and αCD –TMAmC11 hydrogels, which showed longer relaxation times. The obtained relaxation spectra were analysed by the generalized Maxwellian model, which estimates the relaxation modes and the second-order average relaxation time ($\langle\tau\rangle_w$) (Table S11). Although $\langle\tau\rangle_w$ of the αCD-C12 hydrogel was shorter than 2×10^{-3} s, the $\langle\tau\rangle_w$ values of the αCD-ImC11, αCD-PyC11, αCD-VC11, and αCD-TMAmC11 hydrogels were 1.8, 18, and 6.6×10^3, 9.5×10^3 s, respectively. The absence of a cationic unit in the αCD-C12 hydrogel should result in fast threading/dethreading motions with smaller $\langle\tau\rangle_w$ than other species.

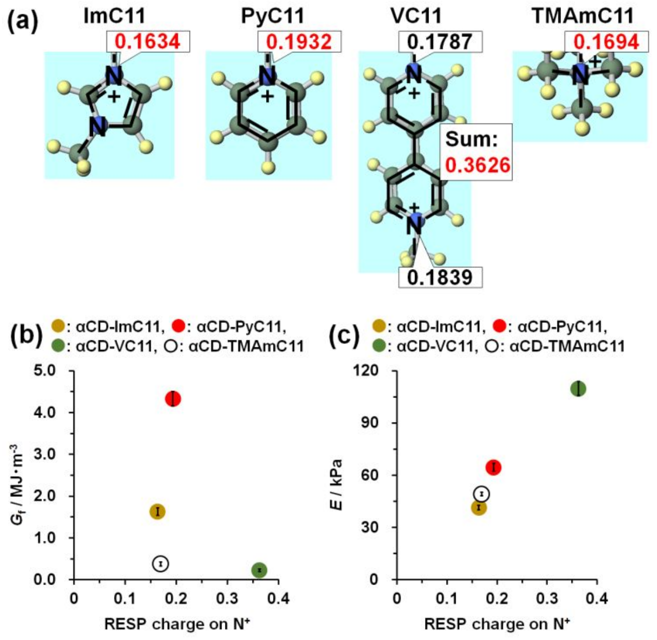

Figure 5. **(a)** The RESP partial atomic charges on N^+ in ImC11, PyC11, VC11 and TMAmC11 monomers. The charges on N^+ are shown in the boxes. **(b)** Plots of G_f and the RESP charges on N^+. (c) Plots of E and the RESP charges on N^+.

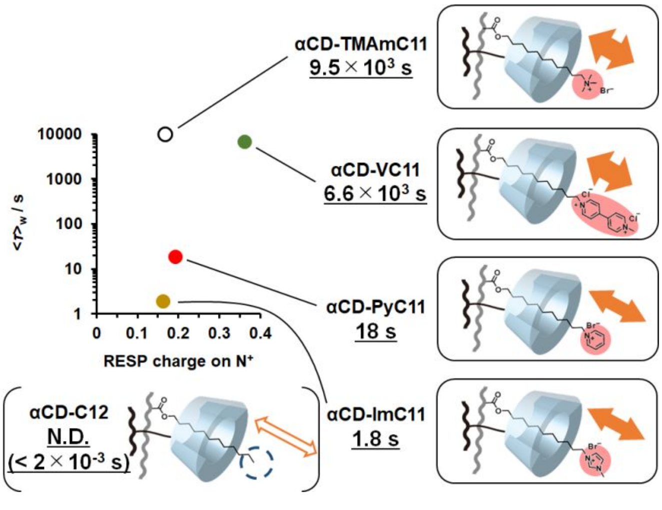

Figure 6. Plots of the second-order relaxation time ($\langle\tau\rangle_w$) and RESP charges on N^+, and schematic of the reversible cross-linking points of the αCD-R hydrogels.

The master curves of the αCD-R hydrogels were evaluated with the sticky reptation model[88,89] (see the Electronic Supporting Information). Figures S41d–45d show theoretical lines for the plateau values from the entanglements (G_e: dotted line). The dashed lines (G_s in Figures S41d–45d) represent those from the entanglements and reversible cross-links (host-guest cross-links). G_e is the experimental rubbery plateau for the entangled polyacrylamide solution[89]. G_s is the theoretical G' derived from the sticky reptation model, in which the entangled polymer network is assumed to be cross-linked by host-guest inclusion complexes as sticking points.

The observed G' of the αCD-R hydrogels increased with increasing ω from G_e to G_s, indicating that the G' value is derived from the entanglement of the polyacrylamide chains and the host-guest interactions. Therefore, the increase in G' is due to the inclusion complexes as sticking points, suggesting that the observed relaxation modes of the αCD-R hydrogels are derived from the association and dissociation of the reversible cross-linking points formed by the inclusion complexes. The αCD-C12 hydrogel did not show distinct relaxation modes, but its G'' was in proportion to $\omega^{0.5}$ in high frequency region, which is derived from the Rouse modes of the polymer network.[90] We estimated the longest relaxation time (τ) of the Rouse modes of the αCD-C12 hydrogel as about 2×10^{-3} s by curve fitting using the generalized Maxwellian model. τ attributed to the host-guest cross-linking points (stickers) should be faster than that of the Rouse modes. Based on these observations and considerations on the relaxation, the calculated $\langle\tau\rangle_w$ is found to be closely related to the lifetime of the reversible cross-linking points.

Figure 6 shows the relation between $\langle\tau\rangle_w$ and RESP charge on N^+ of the cationic unit. $\langle\tau\rangle_w$ linearly increased with the RESP charges on N^+, except for the αCD-TMAmC11 hydrogel. The relation between $\langle\tau\rangle_w$ and the RESP charge supports the above idea of the lifetime of the reversible cross-linking points. The

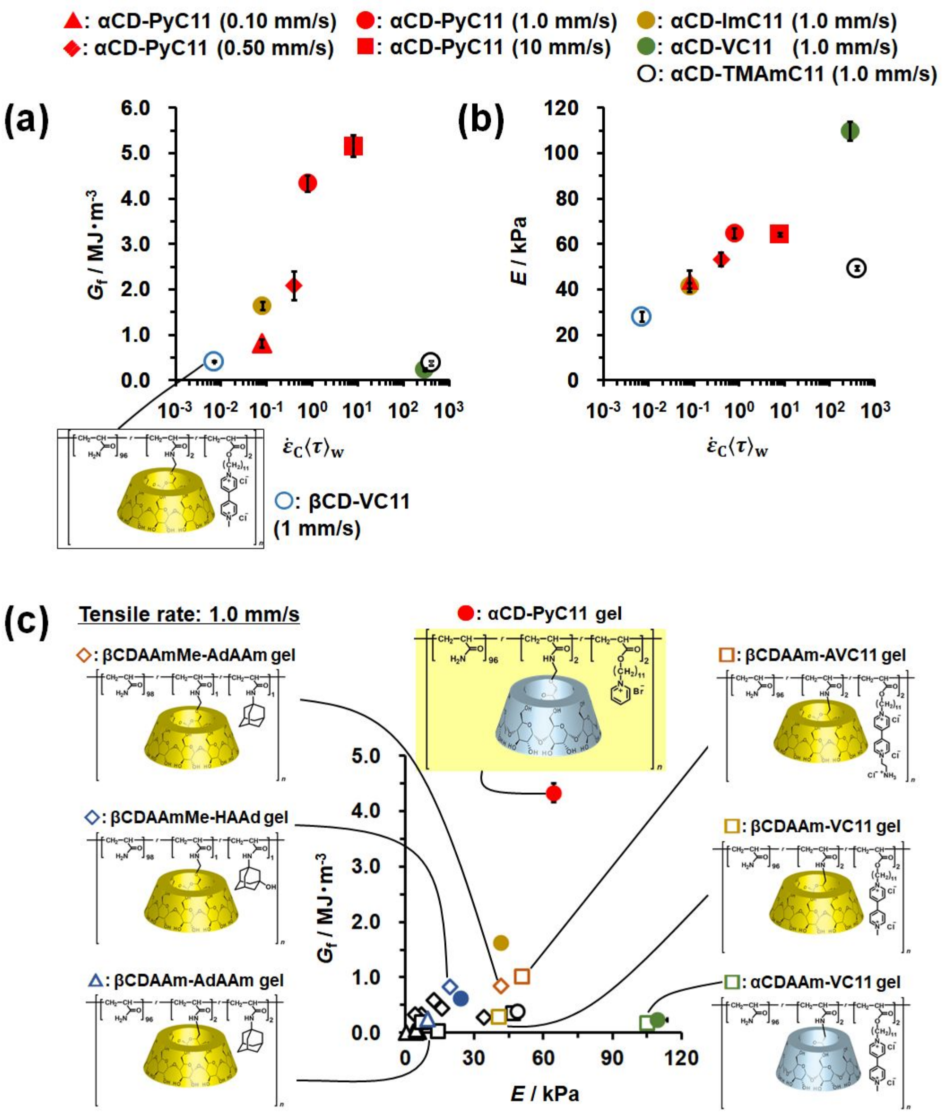

Figure 7. **(a)** Plots of G_f and $\dot{\varepsilon}_C\langle\tau\rangle_w$ of the αCD-R hydrogels. **(b)** Plots of the E and $\dot{\varepsilon}_C\langle\tau\rangle_w$ of the αCD-R hydrogels. The true strain rate decreases with increasing strain. For example, true $\dot{\varepsilon}_C\langle\tau\rangle_w$ at a strain of 1000% will be one-tenth of the initial $\dot{\varepsilon}_C\langle\tau\rangle_w$ **(c)** Plots of G_f and E of the host-guest hydrogels in this work (filled circle) and previous achievements (open triangle,[92] diamond,[93] and square[74]).

αCD-TMAmC11 hydrogel showed the longest $<\tau>_w$ although the RESP charge on N^+ was similar to ImC11. This is mainly attributed to the large steric hindrance effect of TMAmC11 on αCD.

Furthermore, the trend of $<\tau>_w$ of the αCD-R hydrogels is consistent with the following kinetics studies of complexation behaviours of αCD in aqueous solution system. Association/dissociation rates (k_1 and k_{-1}) in complexation with alkyl chains through tricationic[69] or bulky cationic[68,71,72] groups could be determined, because the threading motions are too slow on NMR time scale. On the other hand, complexation through mono- or dicationic groups with low steric hindrance were so fast that k_1 and k_{-1} could not be estimated by NMR spectroscopy.[69,72,91] These results indicate that the kinetics of the threading/dethreading of the CD units directly affected the viscoelastic properties of the αCD-R hydrogels, and that the increment of E accompanied with the RESP charge is attributed to the delay of the viscoelastic relaxation time.

2-6. Relationship between the mechanical properties and the viscoelastic properties of the αCD-R hydrogels

The linear viscoelastic measurements revealed distinct relaxation times derived from the reversible cross-linking points. Figure 7a demonstrates the viscoelastic behaviour of the reversible cross-linking points under tensile testing, showing its relation with G_f. Figure 7b demonstrates the relation between the viscoelastic behaviour and E. The X axis shows the product of $<\tau>_w$ and the nominal strain rate ($\dot{\varepsilon}_C$), which is called as the Weissenberg number: that is a dimensionless parameter that characterizes the behaviour of a viscoelastic body during a deformation process. $\dot{\varepsilon}_C$ is calculated from the tensile speed (v) and initial length of a sample (L_0) as

$$\dot{\varepsilon}_\mathrm{C} \equiv \frac{\mathrm{d}\varepsilon_\mathrm{c}}{\mathrm{d}t} = \frac{\mathrm{d}}{\mathrm{d}t}(\lambda - 1) = \frac{v}{L_0}$$

Figure 7a shows that G_f reached its maximum within $\dot{\varepsilon}_\mathrm{C}\langle\tau\rangle_\mathrm{w}$ of 1~10. At a tensile rate of 1.0 mm/s (circles), $\dot{\varepsilon}_\mathrm{C}\langle\tau\rangle_\mathrm{w}$ of the αCD-ImC11, αCD-PyC11, and αCD-VC11 hydrogels were 0.081, 0.80, and 290, respectively. When $\dot{\varepsilon}_\mathrm{C}\langle\tau\rangle_\mathrm{w}$ of the αCD-R hydrogels was in the range of 1~10, the αCD-R hydrogels acted as viscoelastic bodies. The αCD-R hydrogels with $\dot{\varepsilon}_\mathrm{C}\langle\tau\rangle_\mathrm{w}$ = 1~10 showed high G_f values, indicating that the viscoelastic body showed high G_f. G_f of the αCD-PyC11 hydrogel was dependent on the tensile rate (0.10, 0.50, 1.0, and 10 mm/s). In particular, G_f of the αCD-PyC11 hydrogel was highest (5.2 MJ/m^3) at a tensile rate of 10 mm/s (red square: $\dot{\varepsilon}_\mathrm{C}\langle\tau\rangle_\mathrm{w}$ = 8.0). On the other hand, G_f of the αCD-PyC11 hydrogel drastically decreased at tensile rates of 0.50 mm/s (red diamond: $\dot{\varepsilon}_\mathrm{C}\langle\tau\rangle_\mathrm{w}$ = 0.40) or 0.10 (red triangle: $\dot{\varepsilon}_\mathrm{C}\langle\tau\rangle_\mathrm{w}$ = 0.080), and the hydrogel acted as a viscous body at $\dot{\varepsilon}_\mathrm{C}\langle\tau\rangle_\mathrm{w} < 1$. G_f of the αCD-ImC11 and αCD-VC11 hydrogels decreased outside of range of $\dot{\varepsilon}_\mathrm{C}\langle\tau\rangle_\mathrm{w}$ = 1~10, in which the αCD-ImC11, αCD-VC11 and αCD-TMAmC11 hydrogels acted as the viscous body ($\dot{\varepsilon}_\mathrm{C}\langle\tau\rangle_\mathrm{w} < 1$) and the elastic body ($\dot{\varepsilon}_\mathrm{C}\langle\tau\rangle_\mathrm{w} > 10$), respectively. These results indicate that the linear viscoelastic properties strongly influence the mechanical toughness of the αCD-R hydrogels.

Figure 7b shows the relation between $\dot{\varepsilon}_\mathrm{C}\langle\tau\rangle_\mathrm{w}$ and E. The tensile rate dependence of E for the αCD-PyC11 hydrogel correlated E with the linear viscoelastic spectra. The E of the αCD-PyC11 hydrogel increased with increasing $\dot{\varepsilon}_\mathrm{C}\langle\tau\rangle_\mathrm{w}$ in the range of $\dot{\varepsilon}_\mathrm{C}\langle\tau\rangle_\mathrm{w} < 1$ and reached a steady value at $\dot{\varepsilon}_\mathrm{C}\langle\tau\rangle_\mathrm{w} > 1$. This result is consistent with the ω dependence of G' of the αCD-PyC11 hydrogel (Figure S43d), indicating that the αCD-PyC11 hydrogel acted as a viscoelastic body at $\dot{\varepsilon}_\mathrm{C}\langle\tau\rangle_\mathrm{w} \sim 1$.

Interestingly, in Figures 7a and 7b, we compared the βCD-VC11 hydrogel (blue open circle), which was reported in our previous work,[74,84] with the αCD-R hydrogels by using $\dot{\varepsilon}_\mathrm{C}\langle\tau\rangle_\mathrm{w}$. G_f and E of the βCD-VC11 hydrogel were lower than those of the αCD-ImC11 and αCD-PyC11 hydrogels due to lower $\dot{\varepsilon}_\mathrm{C}\langle\tau\rangle_\mathrm{w}$. In particular, the βCD-VC11 hydrogel, which has the same VC11 guest unit, was a viscous body. On the other hand, as described above, αCD-VC11 acted as the elastic body to show low G_f. This is the opposite result, as it depends on the cavity size of the CDs. This parameter enables us to evaluate various CD-based hydrogels at different tensile rates in a similar way.

Figure 7c shows the relation between G_f and E of the host-guest hydrogels developed in this work and in our previous work as they were strained at 1 mm/s.[74,92,93] The αCD-PyC11 hydrogels achieved higher G_f compared to those of our previous works. G_f of the βCDAAmMe-AdAAm hydrogel was low due to its short τ of stickers (~ 2×10^{-4} s)[89,93], whereas the βCDAAmMe-AdAAm hydrogel has self-healing properties, and the K_a of the βCD-Ad complex is high. G_f and E of the αCDAAm-VC11 hydrogel are similar to those of the αCD-VC11 hydrogel due to the long τ, which is derived from the large potential barrier of the VC11 unit against the αCD unit.

As mentioned above, the kinetics of the threading/dethreading of the CD units strongly influences the lifetime of the reversible cross-linking points. The relationship between the lifetime and the tensile rate drastically changed the G_f and E of the αCD-R hydrogels. Molecular design focusing on the lifetime of the reversible cross-linking points is important to improve the G_f of supramolecular hydrogels.

Conclusions

We prepared five kinds of reversible-cross-linked αCD-R hydrogels (αCD-C12, αCD-ImC11, αCD-PyC11, αCD-VC11, and αCD-TMAmC11 hydrogels) and investigated the relations between the lifetime ($<\tau>_\mathrm{w}$) of the reversible cross-linking points and the mechanical properties (G_f and E). The inclusion complex of the αCD unit and the cation-terminated linear alkyl chain unit on the polymer side chain functioned as a reversible cross-linking point. Quantum chemical calculations and linear viscoelastic measurements revealed that $<\tau>_\mathrm{w}$ was controlled by the kinetics of the threading/dethreading of the αCD units, which was influenced by the potential barrier of the cationic units. We demonstrated the effect of the viscoelastic behaviour of the reversible cross-linking points on G_f of the αCD-R hydrogels using a dimensionless parameter $\dot{\varepsilon}_\mathrm{C}\langle\tau\rangle_\mathrm{w}$. The αCD-R hydrogels exhibited high G_f within $\dot{\varepsilon}_\mathrm{C}\langle\tau\rangle_\mathrm{w}$ of 1~10, where the reversible cross-linking points acted as viscoelastic bodies and G'' of the hydrogels was high. We found that G_f within $\dot{\varepsilon}_\mathrm{C}\langle\tau\rangle_\mathrm{w}$ of 1~10 showed a local maximum because the observed G'' of the αCD-R hydrogels represents the energy dissipated by dissociation of the reversible cross-linking points. In the region of $\dot{\varepsilon}_\mathrm{C}\langle\tau\rangle_\mathrm{w} << 1$, only the entangled polymer network contributes to G_f because the inclusion complexes in the viscous state cannot contribute to energy dispersion. On the other hand, in the region of $\dot{\varepsilon}_\mathrm{C}\langle\tau\rangle_\mathrm{w} > 10$, the inclusion complexes behave like fixed cross-links, resulting in brittleness, similar to a conventional chemically cross-linked network. On the basis of these results, we have to design a molecular structure focusing on relaxation behaviour, *i.e.,* the lifetime of the reversible cross-linking points, to achieve tough materials. Now, we are investigating the design of tough and functional materials using reversible cross-linking with suitable relaxation times.

Conflicts of interest

There are no conflicts to declare.

Acknowledgements

This research was funded by a Grant-in-Aid for Scientific Research (B) (No. JP26288062 & JP18H02035) from MEXT, Scientific Research on Innovative Area Grant Numbers JP19H05718 and JP19H05721 from JSPS of Japan, JST-Mirai Program Grant Number JPMJMI18E3, the Ogasawara Foundation for the Promotion of Science & Engineering, the Murata Science Foundation, and Iketani Science and Technology Foundation. The computations were performed at the Research Center for Computational Science, Okazaki, Japan. We appreciate Dr. N. Inazumi of Osaka University for technical assistance with the NMR measurements. We also want to send our gratitude to the Analytical Instrument Facility, Graduate School of Science, Osaka University.

Notes and references

1 P. J. Flory, *Faraday Discuss. Chem. Soc.*, 1974, **57**, 7–18.

2 J. Alemán, A. V. Chadwick, J. He, M. Hess, K. Horie, R. G. Jones, P. Kratochvíl, I. Meisel, I. Mita, G. Moad, S. Penczek and R. F. T. Stepto, *Pure Appl. Chem.*, 2007, **79**, 1801–1829.

3 I. W. Hamley, in *Introduction to Soft Matter*, John Wiley & Sons, Ltd, 2007, pp. 111–159.

4 E. M. Ahmed, *J. Adv. Res.*, 2015, **6**, 105–121.

5 E. A. Kamoun, E. R. S. Kenawy and X. Chen, *J. Adv. Res.*, 2017, **8**, 217–233.

6 K. Y. Lee and D. J. Mooney, *Chem. Rev.*, 2001, **101**, 1869–1879.

7 S. J. Buwalda, K. W. M. Boere, P. J. Dijkstra, J. Feijen, T. Vermonden and W. E. Hennink, *J. Control. Release*, 2014, **190**, 254–273.

8 U. G. K. Wegst and M. F. Ashby, *Philos. Mag.*, 2004, **84**, 2167–2186.

9 P. Calvert, *Adv. Mater.*, 2009, **21**, 743–756.

10 X. Zhao, *Soft Matter*, 2014, **10**, 672–687.

11 A. K. Means and M. A. Grunlan, *ACS Macro Lett.*, 2019, **8**, 705–713.

12 J. P. Gong, Y. Katsuyama, T. Kurokawa and Y. Osada, *Adv. Mater.*, 2003, **15**, 1155–1158.

13 J. P. Gong, *Soft Matter*, 2010, **6**, 2583–2590.

14 J. Y. Sun, X. Zhao, W. R. K. Illeperuma, O. Chaudhuri, K. H. Oh, D. J. Mooney, J. J. Vlassak and Z. Suo, *Nature*, 2012, **489**, 133–136.

15 J. Li, W. R. K. Illeperuma, Z. Suo and J. J. Vlassak, *ACS Macro Lett.*, 2014, **3**, 520–523.

16 E. Ducrot, Y. Chen, M. Bulters, R. P. Sijbesma and C. Creton, *Science (80-.).*, 2014, **344**, 186–189.

17 K. Sato, T. Nakajima, T. Hisamatsu, T. Nonoyama, T. Kurokawa and J. P. Gong, *Adv. Mater.*, 2015, **27**, 6990–6998.

18 E. Kamio, T. Yasui, Y. Iida, J. P. Gong and H. Matsuyama, *Adv. Mater.*, 2017, **29**, 1–8.

19 K. Haraguchi and T. Takehisa, *Adv. Mater.*, 2002, **14**, 1120–1124.

20 K. Haraguchi, R. Farnworth, A. Ohbayashi and T. Takehisa, *Macromolecules*, 2003, **36**, 5732–5741.

21 H. J. Li, H. Jiang and K. Haraguchi, *Macromolecules*, 2018, **51**, 529–539.

22 K. Haraguchi, S. Shimizu and S. Tanaka, *Langmuir*, 2018, **34**, 8480–8488.

23 K. Haraguchi, Y. Kimura and S. Shimizu, *Soft Matter*, 2018, **14**, 927–933.

24 Q. Wang, J. L. Mynar, M. Yoshida, E. Lee, M. Lee, K. Okuro, K. Kinbara and T. Aida, *Nature*, 2010, **463**, 339–343.

25 W. C. Lin, W. Fan, A. Marcellan, D. Hourdet and C. Creton, *Macromolecules*, 2010, **43**, 2554–2563.

26 A. Harada, J. Li and M. Kamachi, *Nature*, 1992, **356**, 325–327.

27 A. Harada, J. Li and M. Kamachi, *Nature*, 1993, **364**, 516–518.

28 J. Li, A. Harada and M. Kamachi, *Polym. J.*, 1994, **26**, 1019–1026.

29 Y. Okumura and K. Ito, *Adv. Mater.*, 2001, **13**, 485–487.

30 K. Ito, *Polym. J.*, 2007, **39**, 489–499.

31 A. Bin Imran, K. Esaki, H. Gotoh, T. Seki, K. Ito, Y. Sakai and Y. Takeoka, *Nat. Commun.*, 2014, **5**, 1–8.

32 W. Wang, D. Zhao, J. Yang, T. Nishi, K. Ito, X. Zhao and L. Zhang, *Sci. Rep.*, 2016, **6**, 22810.

33 S. Y. Zheng, C. Liu, L. Jiang, J. Lin, J. Qian, K. Mayumi, Z. L. Wu, K. Ito and Q. Zheng, *Macromolecules*, 2019, **52**, 6748–6755.

34 M. Nakahata, S. Mori, Y. Takashima, H. Yamaguchi and A. Harada, *Chem*, 2016, **1**, 766–775.

35 J. Sawada, D. Aoki, M. Kuzume, K. Nakazono, H. Otsuka and T. Takata, *Polym. Chem.*, 2017, **8**, 1878–1881.

36 J. Sawada, D. Aoki, Y. Sun, K. Nakajima and T. Takata, *ACS Appl. Polym. Mater.*, 2020, **2**, 1061–1064.

37 T. Sakai, T. Matsunaga, Y. Yamamoto, C. Ito, R. Yoshida, S. Suzuki, N. Sasaki, M. Shibayama and U. Il Chung, *Macromolecules*, 2008, **41**, 5379–5384.

38 S. Kondo, T. Hiroi, Y. S. Han, T. H. Kim, M. Shibayama, U. Il Chung and T. Sakai, *Adv. Mater.*, 2015, **27**, 7407–7411.

39 W. Wang, Y. Zhang and W. Liu, *Prog. Polym. Sci.*, 2017, **71**, 1–25.

40 X. Yan, F. Wang, B. Zheng and F. Huang, *Chem. Soc. Rev.*, 2012, **41**, 6042–6065.

41 P. Chakma and D. Konkolewicz, *Angew. Chemie - Int. Ed.*, 2019, **58**, 9682–9695.

42 T. L. Sun, T. Kurokawa, S. Kuroda, A. Bin Ihsan, T. Akasaki, K. Sato, M. A. Haque, T. Nakajima and J. P. Gong, *Nat. Mater.*, 2013, **12**, 932–937.

43 F. Luo, T. L. Sun, T. Nakajima, T. Kurokawa, Y. Zhao, K. Sato, A. Bin Ihsan, X. Li, H. Guo and J. P. Gong, *Adv. Mater.*, 2015, **27**, 2722–2727.

44 T. L. Sun, F. Luo, T. Kurokawa, S. N. Karobi, T. Nakajima and J. P. Gong, *Soft Matter*, 2015, **11**, 9355–9366.

45 A. Bin Ihsan, T. L. Sun, T. Kurokawa, S. N. Karobi, T. Nakajima, T. Nonoyama, C. K. Roy, F. Luo and J. P. Gong, *Macromolecules*, 2016, **49**, 4245–4252.

46 T. L. Sun, F. Luo, W. Hong, K. Cui, Y. Huang, H. J. Zhang, D. R. King, T. Kurokawa, T. Nakajima and J. P. Gong, *Macromolecules*, 2017, **50**, 2923–2931.

47 P. Lin, S. Ma, X. Wang and F. Zhou, *Adv. Mater.*, 2015, **27**, 2054–2059.

48 V. Percec, T. K. Bera and R. J. Butera, *Biomacromolecules*, 2002, **3**, 272–279.

49 M. Guo, L. M. Pitet, H. M. Wyss, M. Vos, P. Y. W. Dankers and E. W. Meijer, *J. Am. Chem. Soc.*, 2014, **136**, 6969–6977.

50 S. Abdurrahmanoglu, V. Can and O. Okay, *Polymer (Guildf).*, 2009, **50**, 5449–5455.

51 J. Hao and R. A. Weiss, *Macromolecules*, 2011, **44**, 9390–9398.

52 E. A. Appel, F. Biedermann, U. Rauwald, S. T. Jones, J. M. Zayed and O. A. Scherman, *J. Am. Chem. Soc.*, 2010, **132**, 14251–14260.

53 E. A. Appel, X. J. Loh, S. T. Jones, F. Biedermann, C. A. Dreiss and O. A. Scherman, *J. Am. Chem. Soc.*, 2012, **134**, 11767–11773.

54 J. Liu, C. S. Y. Tan, Z. Yu, Y. Lan, C. Abell and O. A. Scherman, *Adv. Mater.*, 2017, **29**, 1604951.

55 J. Liu and O. A. Scherman, *Adv. Funct. Mater.*, 2018, **28**, 1–6.

56 J. Liu, C. S. Y. Tan, Z. Yu, N. Li, C. Abell and O. A. Scherman, *Adv. Mater.*, 2017, **29**, 1–7.

57 M. Ni, N. Zhang, W. Xia, X. Wu, C. Yao, X. Liu, X. Y. Hu, C. Lin and L. Wang, *J. Am. Chem. Soc.*, 2016, **138**, 6643–6649.

58 B. V. K. J. Schmidt and C. Barner-Kowollik, *Angew. Chemie - Int. Ed.*, 2017, **56**, 8350–8369.

59 G. Sinawang, M. Osaki, Y. Takashima, H. Yamaguchi and A. Harada, *Chem. Commun.*, 2020, **56**, 4381–4395.

60 C. S. Y. Tan, G. Agmon, J. Liu, D. Hoogland, E. R. Janeček, E. A. Appel and O. A. Scherman, *Polym. Chem.*, 2017, **8**, 5336–5343.

61 M. Zhang, D. Xu, X. Yan, J. Chen, S. Dong, B. Zheng and F. Huang, *Angew. Chemie - Int. Ed.*, 2012, **51**, 7011–7015.

62 J. Szejtli, *Chem. Rev.*, 1998, **98**, 1743–1753.

63 A. Harada, *Supramolecular Polymer Chemistry*, Wiley-VCH, Weinheim, 2012.

64 A. Harada, Y. Takashima and M. Nakahata, *Acc. Chem. Res.*, 2014, **47**, 2128–2140.

65 Y. Takashima, Y. Yuting, M. Otsubo, H. Yamaguchi and A. Harada, *Beilstein J. Org. Chem.*, 2012, **8**, 1594–1600.

66 H. Saito, H. Yonemura, H. Nakamura and T. Matsuo, *Chem. Lett.*, 1990, 19, 535–538.

67 H. Yonemura, M. Kasahara, H. Saito, H. Nakamura and T. Matsuo, *J. Phys. Chem.*, 1992, **96**, 5765–5770.

68 D. H. Macartney, *J. Chem. Soc. Perkin Trans. 2*, 1996, **1996**, 2775–2778.

69 Y. Kawaguchi and A. Harada, *J. Am. Chem. Soc.*, 2000, **122**, 3797–3798.

70 Y. Kawaguchi and A. Harada, *Org. Lett.*, 2000, **2**, 1353–1356.

71 W. Herrmann, B. Keller and G. Wenz, *Macromolecules*, 1997, **30**, 4966–4972.

72 T. Oshikiri, Y. Takashima, H. Yamaguchi and A. Harada, *Chem. - A Eur. J.*, 2007, **13**, 7091–7098.

73 A. Harada, H. Adachi, Y. Kawaguchi, M. Okada and M. Kamachi, *Polym. J.*, 1996, **28**, 159–163.

74 Y. Takashima, K. Otani, Y. Kobayashi, H. Aramoto, M. Nakahata, H. Yamaguchi and A. Harada, *Macromolecules*, 2018, **51**, 6318–6326.

75 W. C. Yount, D. M. Loveless and S. L. Craig, *J. Am. Chem. Soc.*, 2005, **127**, 14488–14496.

76 M. J. Serpe and S. L. Craig, *Langmuir*, 2007, **23**, 1626–1634.

77 S. Seiffert and J. Sprakel, *Chem. Soc. Rev.*, 2012, **41**, 909–930.

78 S. C. Grindy, R. Learsch, D. Mozhdehi, J. Cheng, D. G. Barrett, Z. Guan, P. B. Messersmith and N. Holten-Andersen, *Nat. Mater.*, 2015, **14**, 1210–1216.

79 V. Yesilyurt, A. M. Ayoob, E. A. Appel, J. T. Borenstein, R. Langer and D. G. Anderson, *Adv. Mater.*, 2017, **29**, 1–6.

80 W. G. City, *Proc. R. Soc. London. Ser. A. Math. Phys. Sci.*, 1967, **300**, 108–119.

81 Y. Akagi, H. Sakurai, J. P. Gong, U. Il Chung and T. Sakai, *J. Chem. Phys.*, , DOI:10.1063/1.4823834.

82 C. Liu, H. Kadono, K. Mayumi, K. Kato, H. Yokoyama and K. Ito, *ACS Macro Lett.*, 2017, **6**, 1409–1413.

83 T. Kakuta, Y. Takashima, M. Nakahata, M. Otsubo, H. Yamaguchi and A. Harada, *Adv. Mater.*, 2013, **25**, 2849–2853.

84 H. Aramoto, M. Osaki, S. Konishi, C. Ueda, Y. Kobayashi, Y. Takashima, A. Harada and H. Yamaguchi, *Chem. Sci.*, 2020, **11**, 4322–4331.

85 H. Yamaguchi, R. Kobayashi, Y. Takashima, A. Hashidzume and A. Harada, *Macromolecules*, 2011, **44**, 2395–2399.

86 C. I. Bayly, P. Cieplak, W. D. Cornell and P. A. Kollman, *J. Phys. Chem.*, 1993, **97**, 10269–10280.

87 M. J. Frisch, G. W. Trucks, H. B. Schlegel, G. E. Scuseria, M. A. Robb, J. R. Cheeseman, G. Scalmani, V. Barone, B. Mennucci, G. A. Petersson, H. Nakatsuji, M. Caricato, X. Li, H. P. Hratchian, A. F. Izmaylov, J. Bloino, G. Zheng, J. L. Sonnenberg, M. Hada, M. Ehara, K. Toyota, R. Fukuda, J. Hasegawa, M. Ishida, T. Nakajima, Y. Honda, O. Kitao, H. Nakai, T. Vreven, J. J. A. Montgomery, J. E. Peralta, F. Ogliaro, M. Bearpark, J. J. Heyd, E. Brothers, K. N. Kudin, V. N. Staroverov, R. Kobayashi, J. Normand, K. Raghavachari, A. Rendell, J. C. Burant, S. S. Iyengar, J. Tomasi, M. Cossi, N. Rega, J. M. Millam, M. Klene, J. E. Knox, J. B. Cross, V. Bakken, C. Adamo, J. Jaramillo, R. Gomperts, R. E. Stratmann, O. Yazyev, A. J. Austin, R. Cammi, C. Pomelli, J. W. Ochterski, R. L. Martin, K. Morokuma, V. G. Zakrzewski, G. A. Voth, P. Salvador, J. J. Dannenberg, S. Dapprich, A. D. Daniels, Ö. Farkas, J. B. Foresman, J. V. Ortiz, J. Cioslowski and D. J. Fox, *Gaussian 09*, *Revision E.01*, Gaussian, Inc., Wallingford CT, 2009.

88 L. Leibler, M. Rubinstein and R. H. Colby, *Macromolecules*, 1991, **24**, 4701–4707.

89 Y. Kashiwagi, T. Katashima, M. Nakahata, Y. Takashima, A. Harada and T. Inoue, *J. Polym. Sci. Part B Polym. Phys.*, 2018, **56**, 1109–1117.

90 P. E. Rouse, *J. Chem. Phys.*, 1953, **21**, 1272–1280.

91 R. Castro, L. A. Godínez, C. M. Criss and A. E. Kaifer, *J. Org. Chem.*, 1997, **62**, 4928–4935.

92 M. Nakahata, Y. Takashima and A. Harada, *Macromol. Rapid Commun.*, 2016, **37**, 86–92.

93 Y. Takashima, Y. Sawa, K. Iwaso, M. Nakahata, H. Yamaguchi and A. Harada, *Macromolecules*, 2017, **50**, 3254–3261.